Bull. Mater. Sci., Vol. 38, No. 5, September 2015, pp. 1407–1410. © Indian Academy of Sciences.

Er^{3+}–Al_2O_3 nanoparticles doping of borosilicate glass

JONATHAN MASSERA[1], LAETICIA PETIT[2,3], JOONA KOPONEN[3], BENOIT GLORIEUX[4,*], LEENA HUPA[2] and MIKKO HUPA[2]

[1]Tampere University of Technology, Department of Electronics and Communications Engineering, Korkeakoulunkatu 3, FI-33720 Tampere, Finland
[2]Johan Gadolin Process Chemistry Centre, Åbo Akademi University, Biskopsgatan 8, FI-20500, Turku, Finland
[3]nLight Corporation, Sorronrinne 9, FI-08500 Lohja, Finland
[4]CNRS, Université de Bordeaux, ICMCB, 87 Avenue du Dr Schweitzer, F-33608 Pessac, France

MS received 26 November 2014; accepted 22 April 2015

Abstract. Novel borosilicate glasses were developed by adding in the glass batch Er^{3+}–Al_2O_3 nanoparticles synthetized by using a soft chemical method. A similar nanoparticle doping with modified chemical vapour deposition (MCVD) process was developed to increase the efficiency of the amplifying silica fibre in comparison to using MCVD and solution doping. It was shown that with the melt quench technique, a Er^{3+}–Al_2O_3 nanoparticle doping neither leads to an increase in the Er^{3+} luminescence properties nor allows one to control the rare-earth chemical environment in a borosilicate glass. The site of Er^{3+} in the Er^{3+}–Al_2O_3 nanoparticle containing glass seems to be similar as in glasses with the same composition prepared using standard raw materials. We suspect the Er^{3+} ions to diffuse from the nanoparticles into the glass matrix. There was no clear evidence of the presence of Al_2O_3 nanoparticles in the glasses after melting.

Keywords. Glass; optical fibre; IR photoluminescence; nanoparticles; doping.

1. Introduction

The development of materials doped with Er^{3+} ions has been of great interest, as these materials can be used for signal amplification at the wavelength of 1.55 μm corresponding to the telecommunication window (the $^4I_{13/2}$–$^4I_{15/2}$ transition).[1] In the development of optical devices based on rare-earth (RE) ions, the local environment around the RE was found to be of paramount importance for determining the optical properties.[2] While in homogeneous glasses, RE elements tend to cluster in many compositions, glass ceramics have been found to be a valuable alternative media to control the chemical environment of the RE. In fact, these materials combine the mechanical and optical properties of the glass with some advantages of RE-doped single crystals (higher absorption/emission cross-section and longer lifetimes of luminescent levels).[3] The glass ceramics are usually obtained by nucleation and controlled crystallization of the RE-doped glasses. A new modified chemical vapour deposition (MCVD) compatible nanoparticle doping process has been developed to master with higher accuracy of the RE neighbours in fibres independently from the glass composition.[4]

In this paper, we investigate the effect of Er^{3+}–Al_2O_3 nanoparticles doping on the thermal, optical, structural and luminescence properties of borosilicate glasses. The effect of the addition of doped Al_2O_3 as a fused powder primarily in α-phase, from Aldrich, on those properties of the glasses is also discussed.

2. Experimental

2.1 *Glass preparation*

Thirty grams of glasses with the composition xAl_2O_3–$(100 - x)$ $(0.508SiO_2–0.005P_2O_5 – 0.273B_2O_3–0.212Na_2O–0.0025Er_2O_3)$ (mol%) with x = 1.5 and 4.5 were prepared by the standard melt-quenching process (labelled as R-glass1.5 and 4.5, respectively). $NaH_2PO_4·H_2O$ (Merck, 99%), H_3BO_3 (Aldrich, 99.99%), Na_2CO_3 (Sigma-Aldrich, > 99.5%), Al_2O_3 (Sigma-Aldrich, > 99%), SiO_2 (Sigma-Aldrich, 99%) and Er_2O_3 (MV Laboratory, 99.999%) were used as raw materials in the powder form. The batches were first pre-treated at 400°C overnight to decompose the raw materials and successively melted in an ambient atmosphere in a quartz crucible at 1450°C for 30 min. After quenching, the glass was annealed for 3 h at 40°C below its T_g to remove the internal stress induced by the quenching. Finally the glass was cut, ground and polished.

Glasses with the same compositions were prepared using Al_2O_3 nanoparticles doped with Er^{3+}, which were

*Author for correspondence (benoit.glorieux@icmcb.cnrs.fr)

prepared using the protocol described in Jolivet *et al*[5] (labelled as NP-glass1.5 and NP-glass4.5). The preparation of the Al_2O_3 nanoparticles with the composition $85.7Al_2O_3$–$14.3Er_2O_3$ (mol%) implies to first dissolve 60 mM of $Al(NO_3)_3{\cdot}9H_2O$ and erbium acetylacetonate $ErC_{15}H_{21}O_{16}$ in 250 ml of distilled water in stoichiometric proportion and then mix, by magnetic stirring, the whole solution for 30 min. The solution was then heated during 15 days at 100°C in a tight flask. The solution was successively evaporated at 150°C during 5 h and finally heated at 200°C during 10 h in a furnace with a continuous air flow. At this stage, the compounds were single phased corresponding to the boehmite (AlO(OH)) reference [49-0133] as seen in figure 1. The average size of the particles, measured using the Scherrer formula, was ~ (9 ± 2) nm. The particles were heat treated at 1300°C for 5 h. As seen in the XRD pattern (figure 1), the phases present in the samples are corundum Al_2O_3 [10-0173] and $ErAlO_3$ [24-396]. The nanoparticle-doped glasses (NP-glasses) were prepared by mixing the raw materials and the Er^{3+}–Al_2O_3 nanoparticles and then melted the glass batch using the melting process described in the previous paragraph. In order to prepare the glass with $x = 4.5$ with the same amount of Er^{3+} ions and Al_2O_3 (mol%), Al_2O_3 as a fused powder primarily in α-phase from Aldrich was added in the glass batch prior to the melting (labelled as NP-glass4.5).

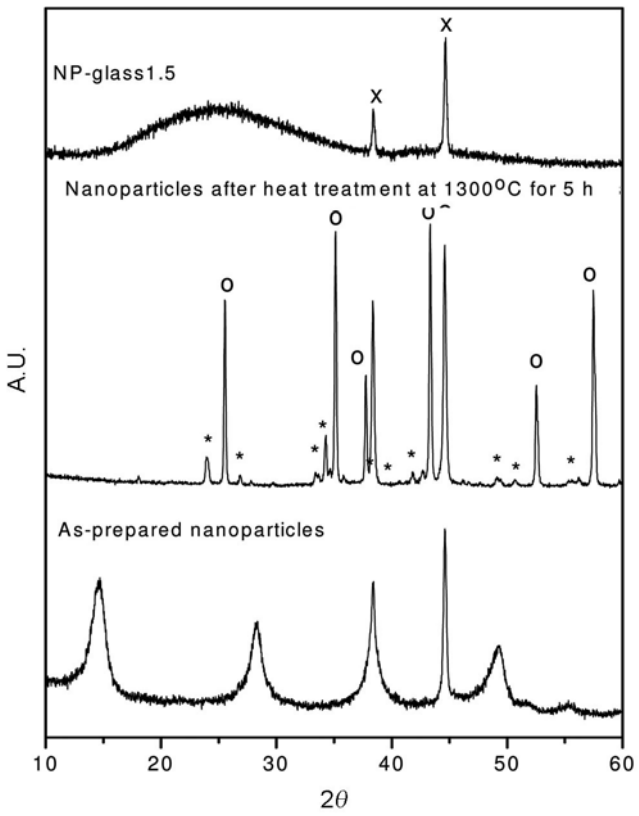

Figure 1. XRD of the heat-treated nanoparticles.

2.2 *Characterizations*

The glass transition (T_g) and crystallization (T_p) temperatures were measured by differential thermal analysis (Mettler Toledo TGA/SDTA851) at a 15°C min^{-1} heating rate. The T_g was taken at the inflection point of the endotherm, as obtained by taking the first derivative of the differential scanning calorimetry (DSC) curve and T_p was defined as the maximum of the exothermic peak. The temperatures were determined with an accuracy of 4°C.

The crystalline phases were identified using an X-ray diffraction analyzer (Philips X'pert) with CuKα radiation (λ = 1.5418 Å). The scans were performed from $2\theta = 0$–60° with a step size of 0.02°.

The density of the bulk glass materials was measured after Archimedes' method in water. The accuracy was better than 0.3%.

The UV–visible–infrared (IR) absorption spectra of the glass samples were recorded using a Perkin Elmer spectrometer over the 250–2500 nm spectral region. The measurements were performed at room temperature and were corrected for the Fresnel losses and the glass thickness.

The emission spectra in the 1400–1700 nm range were measured with an Edinburgh Instruments monochromator (M300) and a liquid nitrogen cooled germanium detector (ADC 403L) at room temperature using an excitation source emitting at 365 nm.

3. Results and discussion

In this paper, we investigate the effect of Al_2O_3 and Er^{3+}–Al_2O_3 nanoparticles on the Er^{3+} luminescence properties of borosilicate glasses. The nanoparticles-doped glasses were prepared using a two-step process: preparation of the Er^{3+}–Al_2O_3 nanoparticles and melting of the borosilicate glass batch which contains the nanoparticles. Al_2O_3 nanoparticles were chosen due to their ability to resist to high temperature and stress condition as suggested by Pastouret *et al*.[6] Alumina is also known to permit high content solubilization of RE ions in a well-dispersed state[1] and can be transformed in a highly thermally resistant phases through appropriate thermal treatment avoiding its destruction during the glass processing.[7]

The density of the glasses and some of their thermal properties are listed in table 1. While the addition of Er^{3+}-doped Al_2O_3 nanoparticles has no impact on the density, T_g and T_p, an increase of the Al_2O_3 content from 1.5 to 4.5 mol% in (regular and NP containing) glasses decreases slightly the density and T_g, but has no strong impact on T_p. It increases ΔT which is an indication of an increase in the resistance of the glass to crystallization. This is in agreement with our previous work.[8] We explained that an increase in the Al_2O_3 content in the glass matrix leads to the formation of negatively charged AlO_4 units, leading to an increase of the Si–BO units in the network. This

Table 1. Density and some thermal properties of the glasses.

Glass code	$[Er^{3+}]$ ($\times 10^{19}$ ions cm^{-3}) (± 5%)	Density (g cm^{-3}) (± 0.02)	Thermal properties		
			T_g (± 4°C)	T_p (± 4°C)	$T_p - T_g$
Glasses with x = 1.5					
R-glass1.5	4.63	2.5	578	727	149
NP-glass1.5	4.63	2.5	580	724	147
Glasses with x = 4.5					
R-glass4.5	4.37	2.47	573	728	156
NP-glass4.5	4.37	2.45	573	735	165

transformation from Si–NBO to Si–BO results from the charge compensation mechanism taking place to neutralize the negative charges of the AlO_4 units.[9] The introduction of Al_2O_3 in borosilicate glasses is also expected to turn the charged four-coordinated boron units into neutral three-coordinated boron. These changes in the glass network result in a reduction of the density and T_g.

The absorption spectra of the investigated glasses were measured and the UV absorption edge was found to remain almost constant at ~ 315 nm, independently of the glass composition. The absorption cross-section at 365 nm is measured from the absorption spectra using

$$\sigma_{abs}(\lambda) = 2.303 \times \log(I_0/I)/(NL) = \alpha(\lambda)/L, \quad (1)$$

where $\log(I_0/I)$ is the absorbance, N the RE ion concentration, L the thickness of the sample and $\alpha_{abs}(\lambda)$ the absorption coefficient.

The absorption cross-section also remains constant at ~ 1.20×10^{-20} cm^{-2} at ± 10% independently of the glass composition. As illustrated in figure 2, no change in the shape of the absorption band can be seen due to the addition of Er^{3+}–Al_2O_3 nanoparticles in both glasses (x = 1.5 and 4.5). However, an increase in the Al_2O_3 content leads to small changes in the absorption band. Similar changes can be seen in the normalized emission band exhibited in figure 3a. This suggests that Al^{3+} ions have a noticeable impact on the crystallographic site of Er^{3+} by modifying the coordination shell of Er^{3+}, in agreement with Bourhis *et al.*[8] However, one can notice that the shape of the emission band of the Er^{3+}–Al_2O_3 nanoparticle-doped glasses with x = 1.5 and 4.5 is similar to that of the regular glasses but is different from the emission recorded directly from the Er^{3+}-doped Al_2O_3 nanoparticles, presented in figure 3b. This tends to indicate that the site of the Er^{3+} in the Er^{3+}–Al_2O_3 nanoparticle-doped glasses (NP-glass1.5 and 4.5) is similar than in the regular glasses (R-glass1.5 and 4.5) prepared using Al_2O_3 as fused powder. A comparison of the relative intensity of the emission at 1530 nm is presented in figure 3c. While the glasses have similar absorption cross-section at 365 nm which corresponds to the excitation wavelength, an increase in the Al_2O_3 content from 1.5 to 4.5 mol% leads to a slight decrease in the intensity of the emission at 1530 nm. As explained in Bourhis *et al*,[8] an increase in the Al_2O_3 content is suspected to increase the content of

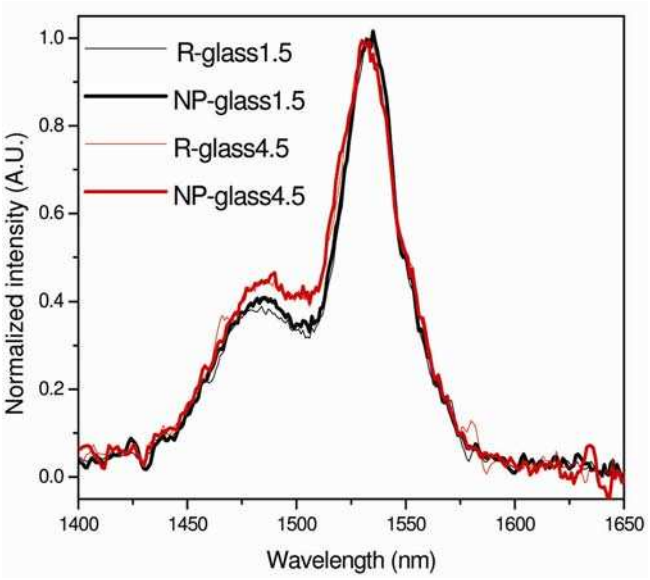

Figure 2. Normalized absorption band of the glasses.

OH hydroxyl groups, well-known to be serious quenchers of Er^{3+} ions luminescence.[10] Surprisingly, no increase in the emission intensity at 1530 nm was observed when the glasses (x = 1.5 and 4.5) were doped with Er^{3+}–Al_2O_3 nanoparticles, while an increased amplifying medium efficiency compared to conventional doped fibres was obtained in silica fibre prepared with similar nanoparticles.[11]

We suspect the Er^{3+} ions to diffuse from the crystalline Al_2O_3 nanoparticles into the glass during the glass melting. We also suspect the Al_2O_3 nanoparticles to decompose inside the glass network as (1) no change in the glass structure was observed using IR and Raman spectroscopies and (2) the sharp peaks of the sample holder were the only peaks seen in the XRD pattern of the Er^{3+}–Al_2O_3 nanoparticle-doped glasses (x = 1.5 and 4.5) as depicted in figure 1 for the NP-glass1.5.

4. Conclusion

Borosilicate glasses with different compositions were prepared to investigate the effect of the glass composition on the Er^{3+} spectroscopic properties. Regular glasses were developed using standard raw materials with two

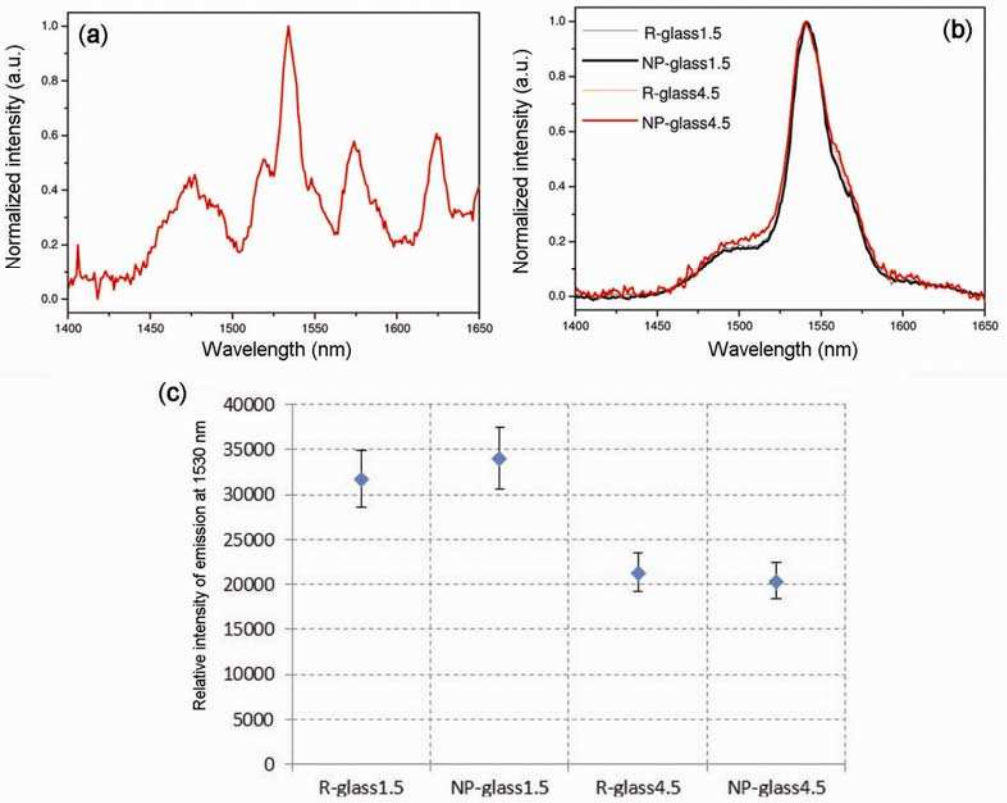

Figure 3. Normalized emission spectra of (**a**) investigated glasses, (**b**) nanoparticles after heat treatment and relative; and (**c**) emission intensity at 1530 nm of the investigated glasses (λ_{exc} = 365 nm).

different concentrations of Al_2O_3 and glasses with the same compositions were prepared using Er^{3+}–Al_2O_3 nanoparticles. While an increase in the Al_2O_3 content had an impact on the Er^{3+} crystallographic site in the borosilicate network, no evidence that the Er^{3+}–Al_2O_3 nanoparticles would remain in the glass after melting was found. From the luminescence properties, the Er^{3+} ions are suspected to diffuse from the nanoparticles into the glass matrix. Compared to previous work on this topic, no enhancement of the Er^{3+} spectroscopic properties was observed in the Er^{3+}–Al_2O_3 nanoparticles containing borosilicate glass. In this paper, it is shown that it is not possible to control the site of the Er^{3+} using nanoparticles doping process in glasses prepared by the standard melting process as compared to the similar work on MCVD compatible nanoparticle doping process.

Acknowledgements

The Academy of Finland is gratefully acknowledged for the financial support to J Massera. The Finnish Funding Agency for Technology and Innovation (TEKES) is acknowledged by nLIGHT for financial support.

References

1. Miniscalo W J 1991 *J. Lightwave Technol.* **9** 234
2. Oppo C I, Corpino R, Ricci P C, Paul M C, Das S, Pal M, Bhadra S K, Yoo S, Kalita M P, Boyland A J, Sahu J K, Ghigna P and d'Acapito F 2012 *Opt. Mater.* **34** 660
3. Dantelle G, Mortier M, Vivien D and Patriarche G 2006 *Opt. Mater.* **28** 638
4. Le Sauze A, Pastouret A, Gicquel D, Bigot L, Choblet S, Jacqueir B, Simonneau C, Bayart D and Gasca L 2003 *Technical digest of OAA 03* (Otara, Japan) Vol. WC 5, p 254
5. Jolivet J P, Froidefond C, Pottier A, Chaneac C, Cassaignon S, Tronc E and Euzen P 2004 *J. Mater. Chem.* **14** 3281
6. Pastouret A, Gonnet C, Collet C, Cavani O, Burov E, Chaneac C, Carton A and Jolivet J P 2009 *Fiber lasers VI: technology, systems, and applications* (*Proc. of SPIE*) Vol. 7195, p. 71951X-1
7. Wilson S J and Mc Connell J D C 1980 *J. Solid State Chem.* **34** 315
8. Bourhis K, Massera J, Petit L, Ihalainen H, Fargues A, Cardinal T, Hupa L, Hupa M, Dussauze M, Rodriguez V and Ferraris M 2015 *Mater. Res. Bull.* **63** 41
9. Kamitsos E I, Kapoutsis J A, Jain H and Hsieh H S 1994 *J. Non-Cryst. Solids* **172** 31
10. Yan Y, Faber A J and de Waal H 1995 *J. Non-Cryst. Solids* **181** 283
11. Podrazky O, Kasik I, Pospisilova M and Matejec V 2009 *Phys. Status Solidi C* **6** 2228